

## Synthesis and characterization of high density polyethylene / peat ash composites

Zhi Cao<sup>a</sup>, Michael Daly<sup>b</sup>, Luke M. Geever<sup>a</sup>, Ian Major<sup>a</sup>, Clement. L. Higginbotham<sup>a</sup>, Declan. M. Devine<sup>a,\*</sup>.

<sup>a</sup> Materials Research Institute, Athlone Institute of Technology, Athlone, Ireland

<sup>b</sup> Mergon International, Castlepollard, Westmeath, Ireland

\*Corresponding author. Address: Declan Devine, Materials Research Institute, Athlone institute of technology, Dublin road, Athlone, Co. Westmeath, N37 F6D7.

Tel: [+353831006225](tel:+353831006225).

E-mail addresses: [ddevine@ait.ie](mailto:ddevine@ait.ie)

Keywords: Peat ash, Stearic acid, High density polyethylene, Compatibilizer

### Highlights

- A new type of polymer composite was developed based on one industrial waste, peat ash, at varying mixing ratios of high density polyethylene.
- The effects of peat ash loading conditions and a coupling agents were studied
- Peat ash composites can generate significant environmental and economic impacts to the automotive reinforce material industries.
- Utilization of peat ash as a filler material in polymer composites may resolve the economic and environmental challenges faced by the peat ash producing industries.

### Abstract

A new type of polymer composite was synthesized from one industrial waste, peat ash, at varying mixing ratios of high density polyethylene (HDPE) and the resulting products were characterized using different experiments included fourier transform infrared spectroscopy (FTIR), scanning electron microscopy (SEM), melt flow index (MFI), density, wettability, tensile test, flexural test and cost analysis. The effects of various ash loads and the use of the maleic anhydride grafted high density polyethylene (HDPE-g-MA) compatibilizer on the physical and mechanical properties of composites were investigated. It was observed that the utilization of peat ash significantly increases the tensile strengths and the flexural modulus, also reduces the cost. Higher peat ash ratios generally lead to higher tensile, flexural strengths and lower cost. Incorporating (HDPE-g-MA) in the composites formulation led to a significant increase in tensile and flexural properties. Conversely, there was a significant decrease of impact strength found for all composites in comparison to the virgin HDPE. And the impact strengths generally decrease as peat ash content increases. Microstructural analysis showed that surface treated peat ash particles appeared to be incorporated into the HDPE matrix as less debonding and voids were observed. In addition, the melt flow ability of the composites decreased remarkably with an increase in peat ash content. No significant water uptake effect was detected on peat ash composites indicating that these materials could be used as a direct

replacement for HDPE in applications where impact strength is not a critical factor. Furthermore, due to the heavier components of peat ash and lack of the voids between filler and matrix, the use of peat ash increased the composite density in comparison to HDPE. Nevertheless, as peat ash reinforcement does offer increased tensile and flexural properties, this may make the end product lighter as lower wall thickness parts can be used to fulfil the same function. From this study, it was concluded that the utilization of the peat ash from peat fired power stations has proved to have significant value-added potential as a filler material in polymer composites.

## Introduction

Peat ash is an industrial waste produced by burning peat primarily for the generation of electricity. Peat is an organic fuel formed through natural atrophy and incomplete disintegration of dead plants under excess humidity and limited air supply conditions [1] and [2]. Peat fuel has many economic and environmental benefits include: (1) energy values equivalent to coal and so it can be used directly as a substitute for coal in power generating stations [1]; (2) low sulphur content and virtually no mercury; (3) cheaper than oil and natural gas and price competitive with other biofuels [1], [2] and [3]. In Finland, peat is used for power generation at power plants ranging in size from 20 to 550 MW, contributing to a total output of over 7000 MW. Similarly, in Russia, more than 6000 MW electric power is produced from peat [2]. In Ireland, peat was the source of heating and cooking for centuries. Peatlands or bogland cover 1.03 million hectares about 15% of the Republic of Ireland. In 2009, 38% of the energy supply was accounted by indigenous fuels like peat [4].

The disadvantage of peat fuel is that it produces large amounts of ash as a waste product [5] and massive amount of peat ash is produced each year [6] and [7]. Peat ash constitutes a major waste problem and the traditional practice mostly involves disposing of it in landfill sites [6] and [8]. However, due to the rise in the cost of waste disposal via landfill and the strengthening of regulations designed to avert an increasing toxic threat to the environment, a new trustworthy and environmentally friendly disposal methods are urgently needed [8] and [9]. To date, although enormous efforts have been made on peat ash deposition reduction and utilization [2], [5] and [10], an economical, widely accepted technology for the recycle and reuse of peat ash has yet to be developed.

The polymer compounding, chemical and coupling agent treatment technologies has recently attracted increasing attention as a viable solution to reusing and recycling industrial ash wastes, which provides a sustainable alternative to landfill of ash, where ash composites have shown beneficial in a variety of applications [11], [12] and [13]. For example, Deepthi et al. [14], studied the mechanical and thermal characteristics of HDPE-fly ash *cenospheres* composites. It was noticed that such composites could be used as potential fire retardants materials. Wang et al. [15] investigated the effects of lightweight fly ash on the microstructure and properties of silica-based composites. From this study, it was reported that the density of the samples decreased as the content of fly ash *cenospheres* increased, while the strength

increased inversely when the content was lower than 50 wt.%. Alfaro et al. [16] study the ionizing radiation effects on polypropylene/ 20% of rice husk ash composites. It was shown that the properties decreased by increasing irradiation dose due to chain scission. The common conclusion by various researchers on polymer-fly ash composites can be formulated: “The content of conventional fly ash in polymer composite compositions enhances their mechanical properties and chemical resistance, in a limited range – exceeding the limit content values (about 12–15% of composite mass for compressive/flexural strength and elasticity modulus where 20% loading has a detrimental effect on tensile strength and workability) [17].”

The composition and properties of ash depend on the type and origin of the fuel used as well as the combustion conditions. Peat as an intermediate product in the formation of coal contains both types of ash formers, namely mineral grains and organically associated ions [18], [19] and [20]. Therefore, the use of coupling agents and chemical treatment to increase the adhesion between fillers and matrix are often necessary [12]. Simple surfactants such as stearic acid can be used as coupling agents in filled polymer systems [12] and [21]. Yao et al. [13], investigated polymer-stearic acid coated fly ash composites. Their study shows that dispersion of fly ash particles in the composites were improved after stearic acid coating due to a reduction in the hydrophilicity of the ash. Sengupta et al. [22], studied the usage of a coupling agent for improving the mechanical and thermal properties of fly ash-recycled PP composites. They concluded that low cost chemicals like stearic acid can be used as an effective coupling agent for fly ash. It has also been reported in literature that the interfacial adhesion between matrix and fillers can also be enhanced by using polymeric coupling agents such as HDPE-g-MA [23], [24] and [25]. Ayswarya et al. [26], concluded that the usage of a compatibilizer consisting of HDPE-g-MA greatly improves the mechanical properties of rice husk ash-HDPE composites. A compatibilized blend was found to have a more homogeneous structure.



**Figure 1.** Utilization Of ash waste filled polymer composites for automobile applications.

Generally, different types of ash waste products are a possible source for polymer composite production. In fact, a great number of ash waste produces have been studied as fillers

**Commented [DD1]:** Environmentally friendly

for composite production, including fly ash [14], [15] and [17], rice husk ash Alfaro et al. [16], bean pod ash [27], oil palm ash [28], carbonized bone ash particulate [29], bagasse ash [30]. More importantly, the fillers play a significant role in the polymer-filler interactions and affect the physical and mechanical properties of the final composite products [31]. Therefore, one of the primary research efforts in the past has been devoted to identify different source materials for polymer composites production and to characterize the properties of the composite products for potential practical applications.

This paper presents an experimental study on the synthesis and characterization of a new type of ash polymer composite derived from an industrial waste, peat ash. The main objectives of this paper were (1) to investigate the potential utilization of the peat ash as reinforce filler for thermoplastic composite production, and (2) to characterize the composition, density, flow ability, moisture level, mechanical properties and cost of the resulting composite products. The effects of various ash loads and the use of the compatibilizer (HDPE-g-MA) on the physical and mechanical properties of composites were also investigated. This study intends to convert industrial wastes into a thermoplastic composite as a beneficial automotive reinforce material.

## **2. Experimental**

### **2.1. Materials**

HDPE [Marlex® HHM 5502BN] used in this study was supplied by Chevron Phillips Chemicals International N.U. Belgium. Raw peat ash was obtained from a Peat-fired power station. The raw ash was subsequently sieved through 355 µm-sieve to remove the large particles and any non-combusted materials. Stearic acid (SA), Sodium hydroxide (NaOH) (99.99% purity), Dicumyl peroxide (DCP) (98 % purity) and maleic anhydride (MA) (95 % purity) were purchased from Sigma Aldrich (Ireland) and used as received.

### **2.2. Peat ash surface treatment**

In this study, 1.5 wt.% of SA was used to surface treated peat ash particles. In order to do this, two separate solutions were prepared. Solution 1 contained 250 ml of 0.01 mol SA and 250 ml 0.014 mol of NaOH. These solutions were mixed at 75 °C until the SA had totally dissolved.

The second solution consisted of 500ml of distilled water which 100 g of peat ash was added at a temperature of 75 °C. Subsequently, these two solutions mixed together at 75 °C for 15 mins. The resultant solution was filtered and the filtrate dried in the oven at 50 °C for 12 hours and stored in an airtight container until required. This process was repeated until enough wet coated peat ash was produced.

### 2.3. Synthesis of HDPE-g-MA compatibilizer

Two wt. % MA and 0.006 wt. % DCP were mixed and ground to a fine-powder using a pestle and mortar. This powder was hand mixed with a 97.994 wt. % powdered HDPE and the mixture was transferred to a feeder fitted with screws of suitable geometry and dimensions for feeding powdered materials. These materials were fed into the APV twin screw extruder and 700 g of the resultant compound was collected for compounding with fillers. Processing conditions for the grafting process is outlined in Table 1.

**Table 1: Processing conditions of maleic anhydride grafted high density polyethylene.**

Reactive extrusion	Zone 1	Zone 2	Zone 3	Zone 4	Die	Speed (RPM)
	170	175	180	190	200	100

### 2.4. Peat ash/ HDPE composites preparation

The compounding of the composites in this study was performed on a Micro 27 laboratory co-rotating twin screw extruder [Leistritz Ltd] with a 27 mm screw diameter and a 38/1 length to diameter ratio. During the compounding process, the temperature profile was increased from 160 °C at the hopper to 200 °C at the die with screw speed of 120rpm utilised.

Peat ash composites were prepared by adding peat ash at loadings of 5, 10 and 20 wt. % to HDPE pellets, fed from a K-tron feeder, at the feed throat of the extruder. HDPE-g-MA/peat ash composites were produced by hand mixing 3 wt. % of HDPE-g-MA with 77 wt. % virgin HDPE for 2 minutes: this mixture was placed in a K-Tron feeder as a substitute for 100% virgin polymer. Another K-Tron feeder was filled with peat ash and the correct feed ratios were set to achieve 95/5, 90/10 and 80/20 polymer-peat ash ratios. These materials were compounded and the resultant composite material was granulated and collected for injection moulding. The composition of high density polyethylene peat ash composites are highlighted in Table 2.

**Table 2: Composition of peat ash-HDPE composites**

Batch	HDPE (wt. %)	HDPE-g-MA (wt. %)	Peat ash (wt. %)
HDPE	100	0	0
PE-A1	95	0	5
PE-A2	90	0	10
PE-A3	80	0	20
PEMA-A1	92	3	5
PEMA-A2	87	3	10
PEMA-A3	77	3	20

#### 2.4.1. Injection moulding conditions

Injection moulding was carried out on an Arburg™ All-rounder 221 K (Table 3) which has a maximum clamping force of 350 kN and a screw diameter of 25 mm. The theoretical stroke volume for this machine is 49 cm<sup>3</sup>. The compounding temperature profile was established by means of four temperature controllers placed along the length of the barrel. A fifth temperature controller was used to regulate the temperature at the nozzle. The mould used was a family type mould producing type “A” test specimens to ISO294-1 and ISO 6239 international standard. The mould used was maintained at 25°C by means of a separate mould temperature controller unit. Settings for injection moulding (dosage stroke, injection speed, injection pressure, holding pressure, back pressure, and cooling time) were optimised for the batches under consideration prior to sample acquisition. All peat ash composite materials were dried for 8 hours at 60 °C prior to injection moulding to remove any moisture retained from the extrusion process. Processing conditions of composites can be seen in Table 3.

**Table 3: Injection moulding settings for all HDPE composites**

	Zone 1	Zone 2	Zone 3	Zone 4	Nozzle	Mould
Temperature (°C)	170	180	190	195	200	25
	Holding time: 6 sec			Back pressure: 50 bar		
	Cooling time: 15 sec.			Injection pressure: 1900 bar		
	Injection speed: 100 mm/s			Holding pressure: 400 bar		

## 2.5. Characterization of surface treatments of the composites

Fourier transform Infrared spectroscopy (FTIR) was performed using a Perkin Elmer Spectrum One FTIR spectrometer. All data was recorded at room temperature, in the spectral range of 650 cm<sup>-1</sup> to 4000 cm<sup>-1</sup>. FTIR have been also used to characterise and compare stearic acid, the SA treated peat ash and the untreated peat ash.

## 2.6. Composite morphology

Scanning electron microscopy (SEM) was performed to identify changes induced by the compatibilizer and SA treatment processes. Freeze-fracture method was implemented in order to observe these changes in the material composite structure. The experiment included the analysis of the uncompatibilized composites and their compatibilized counterpart. Prior to testing, the composite samples (ASTM impact bars) were placed in liquid nitrogen for 10 min before being fractured by a charpy impact machine. After returning to room temperature the composite samples were prepared for SEM, by ensuring that the orientation of the fractured side was correctly placed onto aluminium pin mount adapter using double sided carbon tape. Furthermore, all samples specimens were sputter coated with gold using a Baltec SCD 005 sputter coater to increase the electrical conductivity. Subsequently, A Mira FE SEM was used in high vacuum mode with an acceleration voltage of 15 kV, a resolution of 20 µm and a

magnification of 2.00 k $\times$ , to visualise particle dispersion, utilizing a back scattered electron detector.

## **2.7. Melt flow ability of the composites**

Melt Flow Index was used to identify how well the material flowed under heat and pressure. Melt flow index values of the various samples were measured by using at 190 °C, load 2.16 kg according to the ASTM standard D1238 ( ROSAND Melt Flow Quick Index). The melted material flowed through an orifice of 2.00mm diameter during 10mins and the values were reported in g/10min. Ten specimens per batch were tested and the average melt flow rate was calculated.

## **2.8. Density of the composites**

Prior to density measurements, all samples were dried at 50 °C for 18 hours. To calculate the density of the composites the mass of the sample was recorded using a Sartorius MC201P high sensitivity balance capable of reading to  $\pm 0.0001$ g. The volume of the sample was measured by immersing the sample into a graduated cylinder filled with distilled water and measuring the volume change caused by submerging the sample. Care was taken to ensure that no air bubbles were trapped prior to taking the measurement. Density was calculated by dividing the mass by the volume. Ten specimens per batch were assessed. The average of the ten was calculated as composite density.

## **2.9. Water uptake**

Water uptake test was carried out according to ISO 62:2008. Impact specimens as per ASTM standards were selected and subjected to moisture absorption. The composite specimens to be used for water uptake test were first dried in an air oven at 60 °C for 24 hours and their weight was recorded. These conditioned composite specimens were then immersed in distilled water at room temperature for 7 days. At regular intervals, the specimens were removed from water and wiped with filter paper to remove surface water and weighed with digital balance of 0.01 mg resolution. The samples were re-immersed in water to permit the continuation of water absorption until the saturation limit was reached. The weighing was done within 30 s, in order to avoid errors due to evaporation. After 7 days, the test specimens were again taken out of the water bath and weighed.

## **2.10. Mechanical properties of the composites**

### **2.10.1. Tensile properties**

Tensile tests were carried out using a Lloyd LRX tensometer according to ASTM standard D3039. Composites specimens were mounted and strained at a rate of 2 mm/min until failure occurred. Ten specimens per batch were tested and the average strength was calculated.

### **2.10.2. Flexural properties**

For flexural analysis, a Lloyd LRX tensometer was used in compression mode at a rate of 2 mm/ min with a span of 80 mm in accordance with ASTM standard D790-10. All results

were analysis using NEXYGEN™ software. Ten specimens per batch were tested and the average flexural modulus was calculated.

### 2.10.3. Impact properties

Impact testing was carried out using a Resil 25 Digital Impact Tester, manufactured by Ceast, fitted with a 4 kJ hammer according to ASTM standard D256. A notch of 1 mm was made on each virgin HDPE sample and 0.5 mm was made on each composites sample to ensure failure. Ten specimens per batch were tested and the average fracture energy was calculated. Notched izod impact strength was calculated using Equation 1.

$$\text{Impact strength (KJ/m}^2\text{)} = (W/h \times b_N) \times 10^3 \quad (1)$$

Where W is the corrected energy in J, absorbed by breaking the test specimen; h is the thickness, in mm, of the test specimen;  $b_N$  is the remaining width, in mm, at the notch base of the test specimen

### 2.11. Raw material cost

The actual cost of the composite was determined based on the composition of each component. The weight percentage of peat ash and HDPE content was calculated gravimetrically according to ASTM D2734 (ASTMD2734-09). The composite specimens to be used for cost analysis were first dried in an air oven at 60 °C for 24 hours and their weight was recorded. Then, the weighed sample was placed into a weighed crucible and burned in a 500°C muffle furnace for 30 mins until only the peat ash remains. The crucible was cooled and weighed. The HDPE and peat ash contents were calculated as a weight percent from the available data. For cost analysis purposes, the price for HDPE and peat ash were taken at the euro per kg, the cost of HDPE was assumed to be € 1.3 per kg, peat ash was assumed to be € 0 per kg, SA was assumed to be €1.61 per kg and HDPE-g-MA was assumed to be €1.5 per kg. The extra labour energy and surface treatments costs were not take into account.

$$C_A = P \times R/100 + p \times r/100 + p_s \times r_s/100 + P_M \times R_M/100 \quad (2)$$

Where  $C_A$  is the cost of composite, P is the cost of HDPE, p is the cost of peat ash, R is HDPE weight %, r is peat ash weight %,  $p_s$  is the cost of stearic acid,  $r_s$  is stearic acid weight %,  $P_M$  is cost of HDPE-g-MA,  $R_M$  is HDPE-g-MA weight %.

### 2.12. Statistical analysis

A statistical comparison of the density, water absorption, melt flow index, tensile strength, flexural modulus, impact strength and the actual cost of the composite was performed. Following assessment of normality of distribution and homogeneity of variance, treatments were compared using a one way ANOVA with a Tukey's Honesty Significant Difference Post hoc test to determine differences between individual batches. Differences were considered significant when  $p \leq 0.05$ . To perform this analysis, the IBM SPSS statistics version 19 software was used.



### 3. Result and discussion

#### 3.1. FT-IR spectroscopic analysis

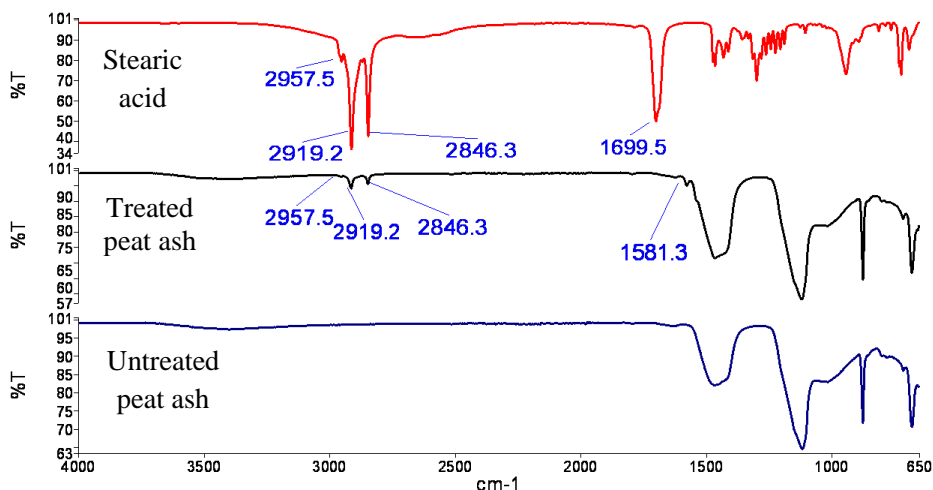


**Figure 2:** FTIR spectra of stearic acid, treated peat ash and untreated peat ash.

The formation of stearic acid monolayer by interaction of their carboxylate group with peat ash on the surface was confirmed by FTIR spectroscopy. Figure 2 shows FTIR spectra of stearic acid, treated peat ash and untreated peat ash. In stearic acid and treated peat ash spectrum, the absorption peaks at  $2919.2\text{ cm}^{-1}$  and  $2846.3\text{ cm}^{-1}$  corresponding to C-H single bonds asymmetric stretching vibration and symmetrical stretching vibration, respectively, helped to identify CH<sub>2</sub> group of SA [32]. The CH<sub>3</sub> group was recognized by asymmetric stretching vibrations of C-H peaks which occurred mainly at  $2957.5\text{ cm}^{-1}$  as reported by Yao et al. [13]. The characteristic peak for the stearic acid occurs in the range of  $1699.5\text{ cm}^{-1}$  cannot be seen in the treated peat ash spectrum. This indicates that the -COOH has undergone chain scission to participate in reactive blending of peat ash. In the treated peat ash spectrum, the presence of absorption bands of COO<sup>-</sup> which occurred at the  $1581.3\text{ cm}^{-1}$  indicate that COO<sup>-</sup> were chemically bonded to the surface of peat ash, and therefore the peat ash microstructure surface might be covered by a monolayer of organic molecules with their nonpolar tails exposed to air [32] and [33]. These observations prove that physical chemistry reaction took place between stearic acid and peat ash surface which varied peat ash surface properties.

#### 3.2. Composite morphology

Figure 3a and 3b illustrates the micro-morphological features of peat ash particles before and after surface treatment. Peat ash (which was dried and sieved through 355  $\mu\text{m}$ -sieve)

is characterized by irregularly shaped aggregates that appear to be porous and comprised of much smaller particles. In fact, mineral grains, the major solid constituent of the peat ash [18]. Thus the aggregates are most likely mineral grains. Moreover, some observable plate-shaped particles, which are believed to be inherited from the original structure of organically associated substrates. Figure 3a2 and 3b2 shows a closer view of peat ash particles. Knowing the SA surfactant coats on the surface of peat ash particles can give contribution to the superior light reflecting quality of the particles. The SA layers decrease of particle-particle interaction and increase adhesion of matrix/ filler. Similar phenomenon were exhibited by Nath et al. [34] when fly ash filler particles were modified by sodium lauryl sulphate.

Figure 3c and 3d illustrates the SEM micrographs of the uncompatibilized composites and their compatibilized counterparts. It is observed that surface treated peat ash particles appeared to be incorporated into the HDPE matrix as less debonding and voids were observed. Compare to compatibilized composites, uncompatibilized composite (Figure 3c) appeared to have formed agglomerates and exhibited poor intimate contact with HDPE matrix, which resulted in debonding between peat ash and the matrix. This effect is as a result of detachment of the unembedded particles during fracture in liquid nitrogen, indicating that there is poor adhesion between the filler and the matrix. The compatibilized composite Figure 3d shows a quasi-brittle fracture surface with matrix undergoing significant deformation prior to debonding of particles which have resulted in a large number of voids. This is due to improved interfacial adhesion leading to resistance offered by matrix for cavitation of particles [35]. This is in agreement with the findings of Igarza et al. who reported that the incorporation of maleic anhydride functionalized polypropylene increased interfacial adhesion between polypropylene and fly ash [36].

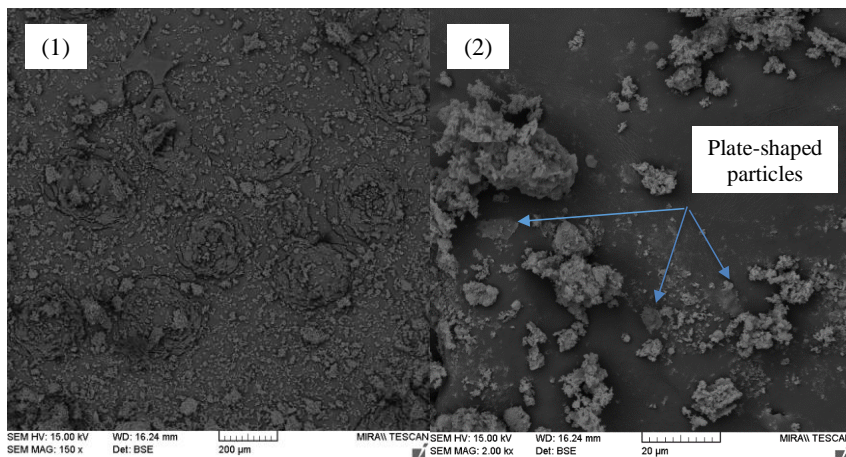


**Figure 3a:** Untreated peat ash.

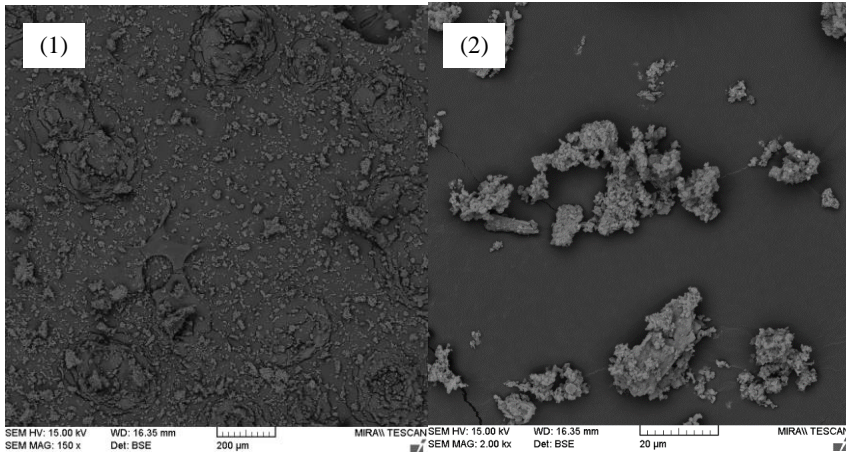


**Figure 3b:** Stearic acid treated peat ash.

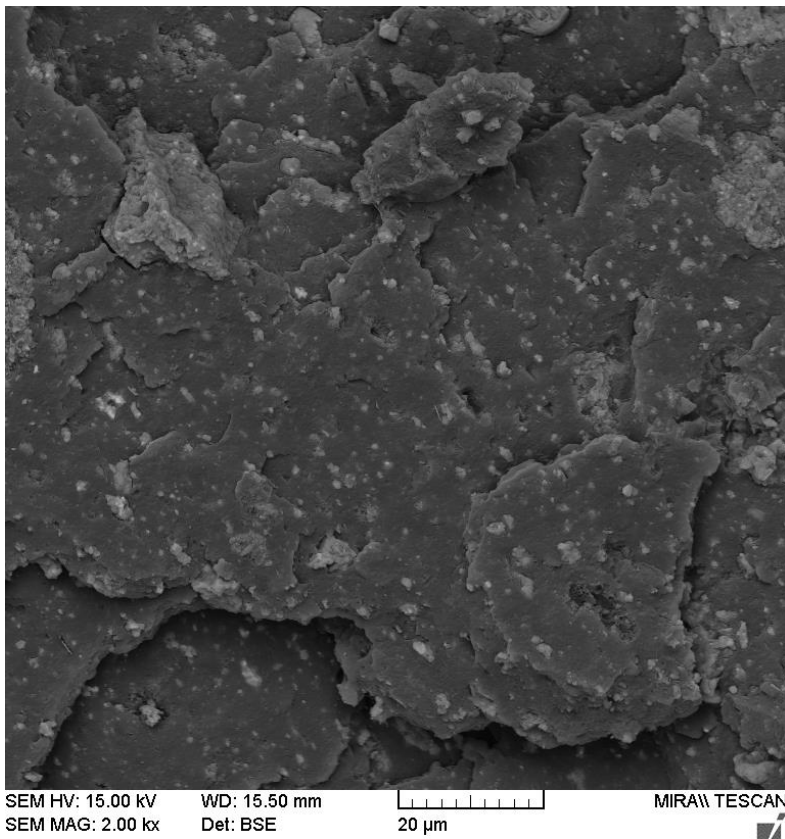


**Figure 3c:** Uncompatibilized composites loaded with 20% SA treated peat ash.

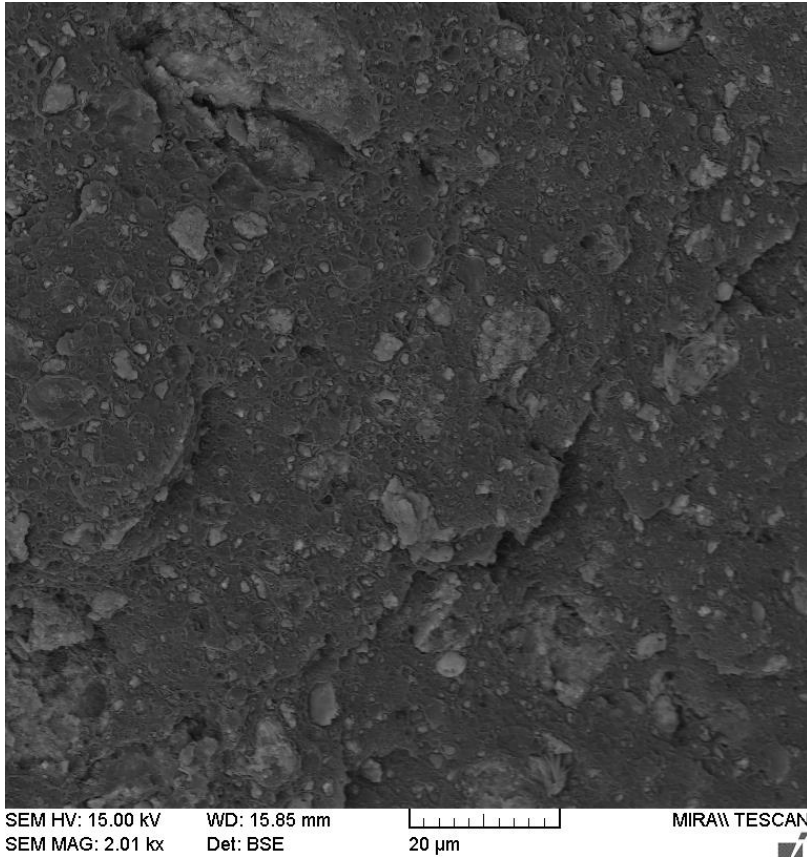


**Figure 3d:** Compatibilized composites loaded with 20% SA treated peat ash.

### 3.3. Density comparison

The density of peat ash composites exhibited an increase in comparison to HDPE values (Figure 4). The results clearly indicated that as peat ash loading increased, the density of composites also increased. Based on the density measurements of the composites, it was found that all the peat ash-HDPE composites had a significantly higher density than that of virgin HDPE ( $p \leq 0.001$ ). 20 wt. % ash loaded composites (PE-A2, PEMA-A2) had a significantly higher density than 10% and 5 wt. % ash loaded composites (PE-A, PEMA-A, PE-A1, PEMA-A1) ( $p \leq 0.05$ ). 10 wt. % ash loaded composites (PE-A1, PEMA-A1) had a significantly higher density than 5 wt. % ash loaded composites (PE-A, PEMA-A) ( $p \leq 0.05$ ).

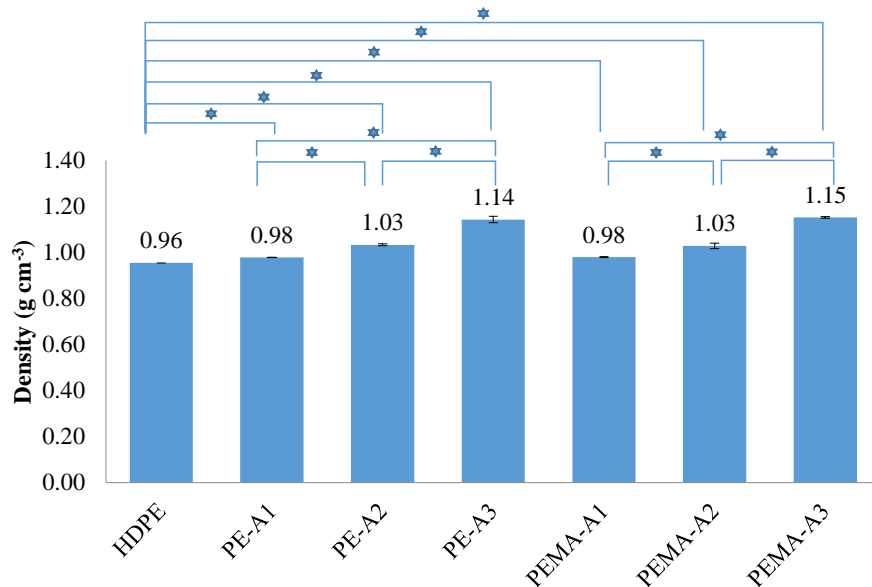


**Figure 4:** Density of HDPE composites made with the various concentrations of peat ash.

★ Denotes a significant difference  $p < 0.05$ .

Ash forms at high temperatures, the compositions of ash is strongly dependent upon the fuel sources being burned (coal, oil, natural gas, peat and biomass, etc.) [37]. Similar to coal ash, peat ash also comprises solid particles and *cenospheres* [18] and [20]. *Cenospheres* are a naturally occurring by-product of the burning process [14]. They are inert hollow silicate spheres and have a low density of about  $0.6 \text{ g/cm}^3$  [14] and [38]. Solid particles ash has a density in the range of  $2.0\text{--}2.5 \text{ g/cm}^3$  [38]. It is therefore conceivable that the average density of all the peat ash was higher than that of HDPE. This led to the composites of peat ash having a higher density than HDPE.

Results also indicate that as peat ash loading increased, the density of composites increased. This may be due to the good compatibility of surface treated peat ash and HDPE matrix. The stearic acid surface coating of ash increased the extent of dispersion and interfacial interaction between ash and polymer matrix [13]. This had led to decrease the voids caused by debonding of the rigid polar particles in the polyolefin composite [39].

### 3.4. Melt flow index (MFI)

Melt flow index analysis was used to determine the ease of flow of peat ash-HDPE composite materials. The MFI value is a parameter that plays an important role in the plastics industry. It allows for direct comparison the molten flow rate of materials. It is dependent on molecular weight, additives, and viscosity of the material under investigation [40]. The standard MFI values for virgin and composites samples used in this study are shown in Figure

5. A general decrease in the melt flow rate of the composites was observed when compared with virgin HDPE. Based on the MFI results, it can be seen that all the peat ash composites had significantly lower melt flow rates compared to virgin HDPE ( $p \leq 0.001$ ) except for batch PE-A, which contained 5 wt. % peat ash ( $p \geq 0.696$ ).

Results also show that as peat ash loading increases, the MFI values of composites decreases. For 5 wt. % ash loaded composites, batch PE-A have a significantly higher MFI than 20 wt. % ash loaded composites (PE-A2) ( $p \leq 0.001$ ). The addition of the *compatibilizer* in sample PEMA-A yielded a significantly higher MFI than 10 wt. % and 20 wt. % ash loaded composites (PEMA-A1, PEMA-A2) ( $p \leq 0.001$ ). For 10 wt. % ash loaded composites, batch PE-A1 had a significantly higher MFI than 20 wt. % ash loaded composites (PE-A2) ( $p \leq 0.001$ ). The addition of the *compatibilizer* batch PEMA-A1 has a significantly higher MFI than 20 wt. % ash loaded composites (PEMA-A2) ( $p \leq 0.001$ ).

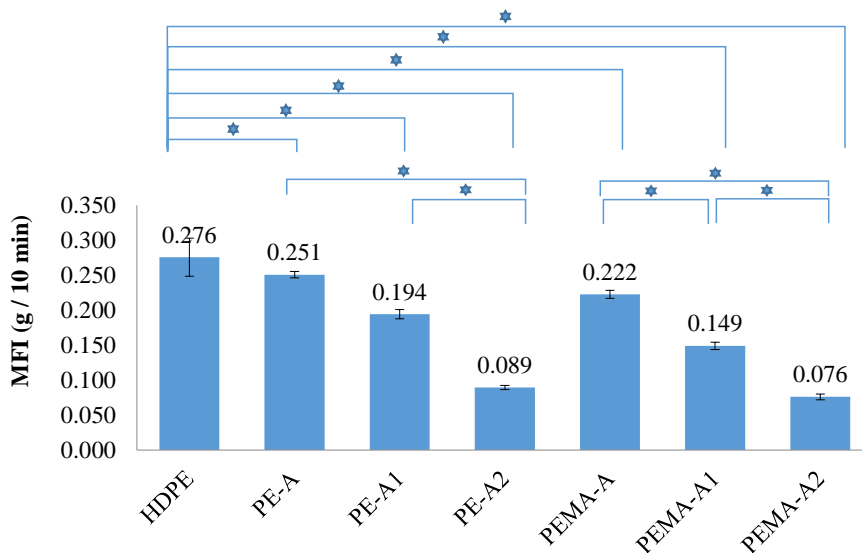


**Figure 5:** Melt flow index of different peat ash composite batches at 200°C with 2.16kg.

★ Denotes a significant difference  $p < 0.05$ .

The results demonstrate large contribution of filler content to the composites melt flow. Ash loading had a significant effect on the flowability (MFI) of the materials tested. These results can be directly related to the un-deformability of the filler and its lack of contribution to the flow [41]. Similar results were obtained by Ayswarya et al. [26], when using rice husk ash-HDPE composites.

Our early studies have shown that the average density of all the components of peat ash is higher than HDPE. Jikan et al [42], also concluded that the use of higher density materials

as fillers could affect the melt flow ability of the composites. additionally, low MFI value indicates a higher melt viscosity [26]. Hence, the addition of peat ash increased the viscous and elastic response of the composites.

### 3.5. Water uptake analysis

Water sensitivity is another important criterion for many practical applications of polymer composite products. Dhakal et al. [43], proposed that water absorption is a major factor affecting the long term strength of polymer matrix. Water absorption behaviour of peat ash-HDPE composites in water at room temperature was studied as per ISO 62: 2008. In Figure 6, the results of water uptake of peat ash-HDPE composite after 24 hours and 7 days are shown. In all peat ash composites, water absorption analysis indicated that the weight of composites was not significantly affected following immersion in water for 24 hours and 7 days at room temperature ( $p \geq 0.05$ ).

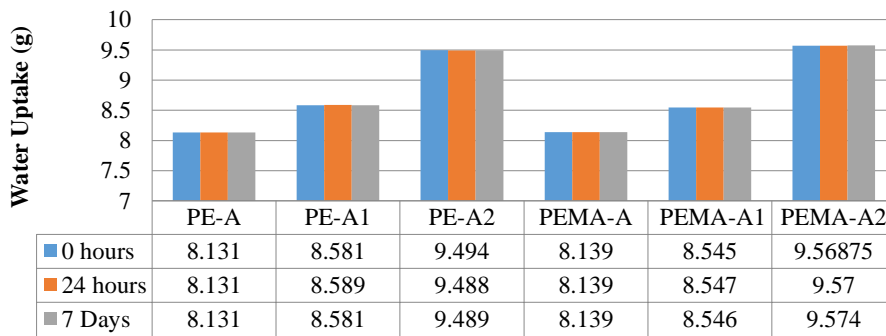


**Figure 6:** Weights of peat ash/ HDPE composites materials after immersion in water for 0, 1 and 7 days at room temperature.

Hence it can be said that water absorption studies of peat ash composites had a marginal effect of moisture uptake. This expected behaviour was mainly due to the *hydrophobic* characteristics of ash and HDPE. Peat ash composite products exhibits excellent water repellent properties, due to the good compatibility between the surface treated peat ash and HDPE matrix. The stearic acid surface treatment significantly increased the extent of dispersion and interfacial interaction between ash and polymer matrix [13], thus preventing the generation of voids in the composites [39]. This water-tight structure further improved water resistant property of peat ash-HDPE composites. Similar results were obtained by Ma et al. [44] in Fly ash-reinforced thermoplastic starch composites.

### 3.6. Mechanical properties

#### 3.6.1. Tensile and flexural properties

Tensile and flexural properties are important characteristics of the stiffness of materials. Figure 7 and Figure 8 display the tensile and flexural properties of the HDPE matrix and peat ash-HDPE composites at room temperature. A general increase in the tensile strength and

flexural modulus of the composites were observed when compared with virgin HDPE. It is found that all the peat ash composites had significantly higher tensile strength and flexural modulus compared to virgin HDPE ( $p \leq 0.001$ ). Except batch PE-A, which contained 5 wt. % peat ash without *compatibilizer* and showed no significant difference in the tensile strength compared to HDPE ( $p \geq 0.07$ ). The reason behind this statistical increase in tensile strength and flexural modulus was likely to be due to the formation of interfacial interactions between filler and matrix playing a significant role in the improvement of tensile and flexural properties compared to the neat polymer. *Hydrophobic* ends of SA molecules on the surface of the ash were adsorbed on the surface of polymer and formed the strong interfacial interactions, which contributed to restrict the mobility of the polymer chains and the effect of stress concentration [13].

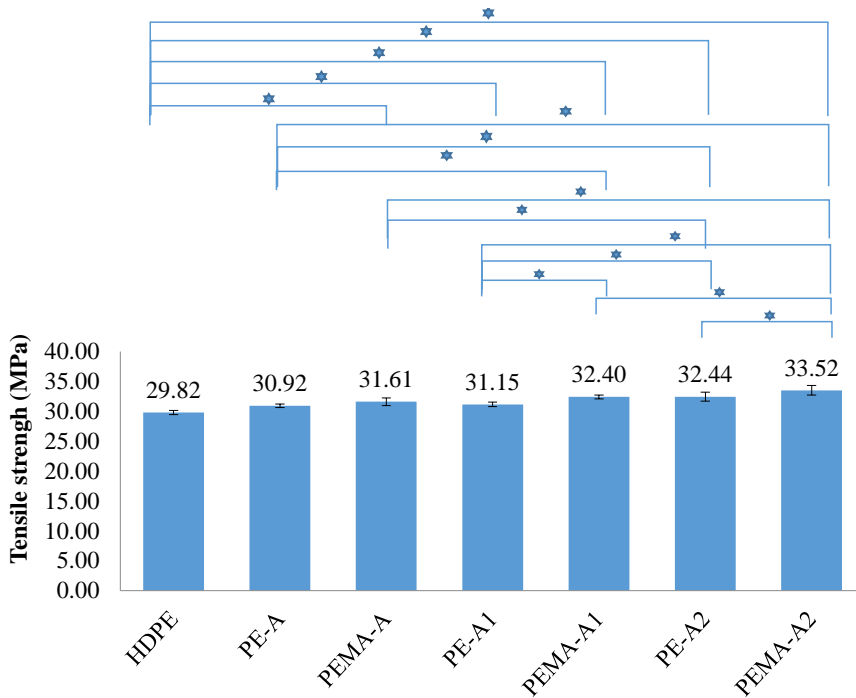


**Figure 7:** Tensile strength of different peat ash/ HDPE composite.

★ Denotes a significant difference  $p < 0.05$ .



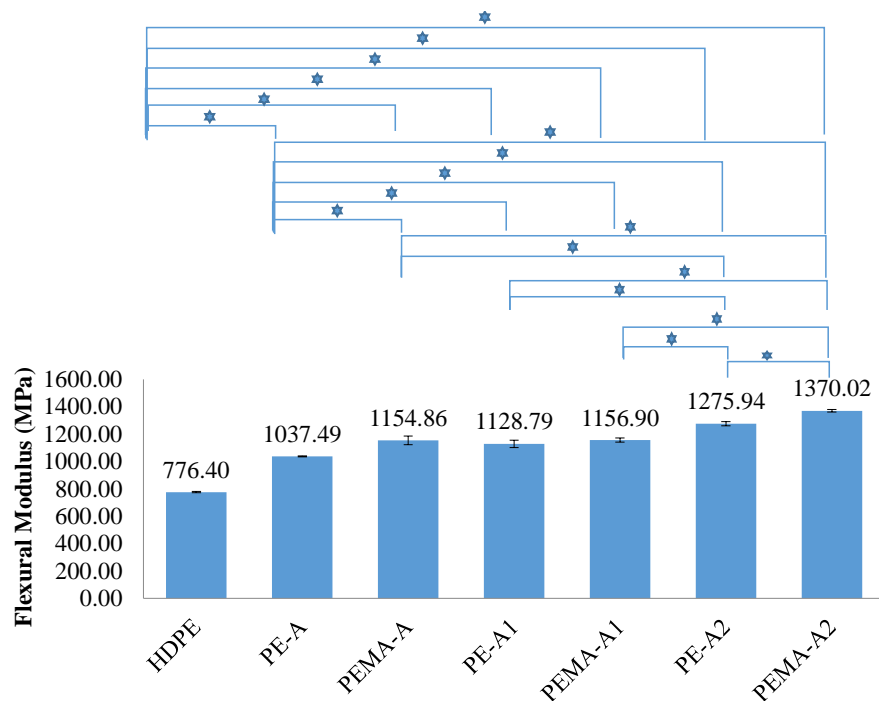


**Figure 8:** Flexural modulus of different peat ash/ HDPE composite.

★ Denotes a significant difference  $p < 0.05$ .

Results have also illustrated that ash content has a significant effect on tensile and flexural properties, as ash loading increase; the tensile and flexural properties of composites improved. Indeed 5 wt. % ash loaded composites, batch PE-A had a significantly lower tensile strength and flexural modulus than 10 wt. % and 20 wt. % ash loaded composites (PE-A1 and PE-A2) ( $p \leq 0.02$ ). The addition of 5 wt. % ash compatibilized composite (PEMA-A) resulted in a significantly lower tensile strength compared to 20 wt. % ash loaded compatibilized composites (PEMA-A2) ( $p \leq 0.001$ ). Similarly, for 10 wt. % ash loaded composites, batch PE-A1 and PEMA-A1 had a significantly lower tensile strength and flexural modulus than 20 wt. % ash loaded composites (PE-A2, PEMA-A2) ( $p \leq 0.02$ ). This behaviour has been described in similar studies and has been explained by the increase of the interfacial area with higher modulus filler content [17], [45], [46] and [47]. The stiffness of these ash polymer composites is dependent on the ability of the polymer to transfer the stress from the polymer matrix to the load bearing filler [48]. As this interfacial area increases, the better interaction between the filler and matrix, hence providing better load transfer from the matrix to the reinforcement [49].

Furthermore, incorporation of HDPE-g-MA into the composites formulation led to a significant increase in tensile and flexural properties. The addition of the *compatibilizer* HDPE-

g-MA (PEMA-A1 and PEMA-A2) resulted in a significantly higher tensile strength and flexural modulus compared to the samples without *compatibilizer* (PE-A1 and PE-A2) ( $p \leq 0.04$ ). In general, the reinforcement mechanisms for polymer composites are closely related to the compatibility and the interfacial adhesion strength between the components [50]. The presence of MA generally increases the interaction between polymers and filler resulting in a better dispersion of the filler and better adhesion between the filler and the polymer [51] [52]. This result successfully verified the use of the *compatibilizer* were effective in enhancing the dispersion, adhesion and compatibility of the filler with the *hydrophobic* matrix [46], [53] and [36].

### 3.6.2. Impact strength

Figure 9 displays the impact properties of the virgin HDPE and peat ash composites at room temperature. Fully brittle behaviour was exhibited for all composite materials. Results have shown all the peat ash composites had significantly lower impact strength compared to virgin HDPE ( $p \leq 0.001$ ). Impact strength generally decreases as peat ash content increases. At 5% ash loaded composites, batch PE-A and PEMA-A had a significantly higher impact strength than 20 wt. % ash loaded composites (PEMA-A2) ( $p \leq 0.001$ ). For 10 wt. % ash loaded composites, batch PE-A1 and PEMA-A1 had significantly higher impact strength than 20 wt. % ash loaded composites (PE-A2, PEMA-A2) ( $p \leq 0.01$ ).

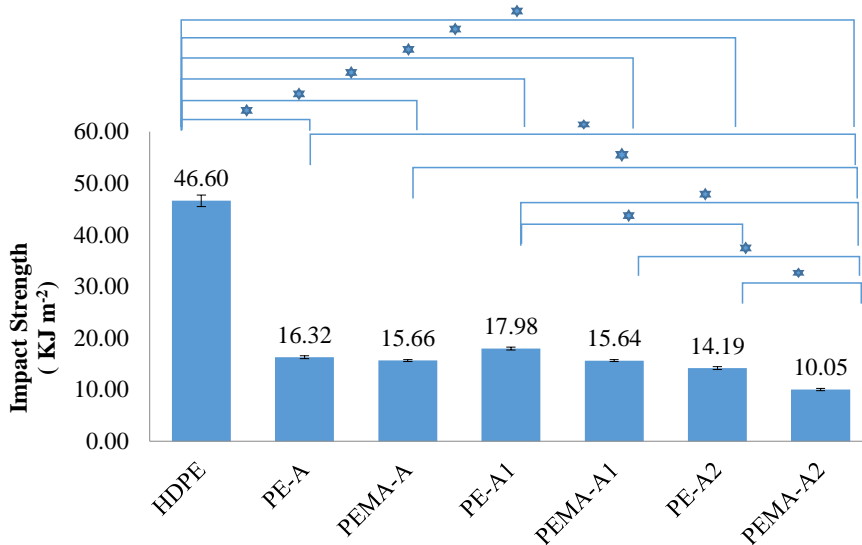


**Figure 9:** Impact strength of different peat ash/ HDPE composite.

★ Denotes a significant difference  $p < 0.05$ .

This phenomenon may be due to the process of plastic deformation of the matrix. Ash composite materials when subjected to impact type of loading conditions, energy is absorbed in the process of plastic deformation of the matrix [36] and [54]. The crack propagates through the matrix with little or no plastic deformation and in front of the crack tip is subjected to plane-strain conditions [55]. This process of deformation is imposed by irregular particle shape and size of rigid ash particles [36] and [56]. Fly ash particles decreased the elasticity of the matrix and led to easy crack initiation along with brittle composites [54], [56] and [57]. Similar phenomenon was exhibited by Parvaiz et al. [56] when fly ash were added to polyetheretherketone composites.

### 3.7. Cost analysis

The primary goal of adding fillers is to lower the overall materials cost of the composite compared to the unfilled polymer [39]. The incorporation of peat ash into HDPE reduces its cost by more than 19%. Materials cost generally decreases as peat ash content increases. When the cost of compatibiliser is considered, these costs of the composites reduce to between 1.3 and 15.9% (Figure 10).

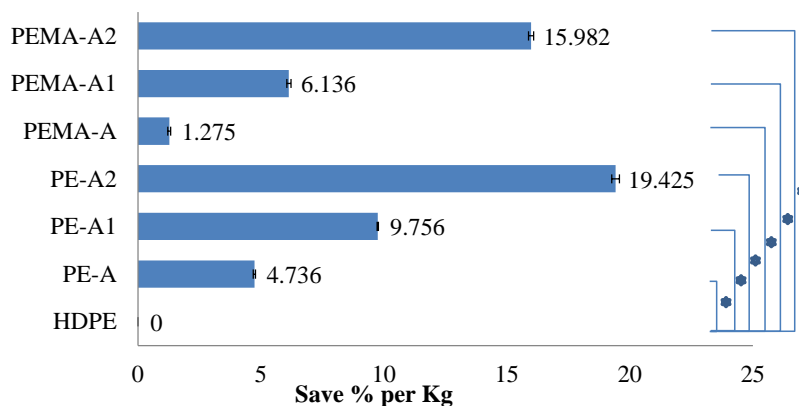


**Figure 10:** Cost comparison of composite materials compared with virgin HDPE.

★ Denotes a significant difference  $p < 0.05$ .

As the raw materials used in the production of HDPE-g-MA are relatively expensive, the use of these compatibilisers in the production of HDPE peat ash composites does affect the final price. As shown in Figure 10, the price per kg decreases upon addition of HDPE-g-MA. However, making good composites is all about knowing how to find a good balance of properties at the lowest cost [58]. The price differences are however still substantial when compared with virgin HDPE. As peat ash also offer the greatest reinforcement they may make the end product more economical as smaller parts could fulfil the required function. The limitation of the cost calculation is the extra labour and energy costs were not taken into

account. However these vary considerably between producers and users therefore the extra costs were ignored.

#### 4. Conclusions

This paper presents an experimental study that aimed to convert an industrial waste, peat ash to a potentially useful automotive reinforce material via polymer processing and compounding technology, resulting in a new type of peat ash/ HDPE composites. A variety of factors, including peat ash loads and the use of the compatibilizer were examined to understand their influence on the physical and mechanical properties of the final products. The microstructure of the end products were also characterized by SEM. Based on the experimental results and observations, the following conclusions can be drawn:

- Utilization of chemical treated peat ash as a filler material in polymer composites reduced the raw material cost provides a simple, effective and economical means of peat ash recycling.
- The studied composites have tensile strengths and flexural modulus of up to 33.52 MPa and 1370.02 MPa, which are significantly higher than virgin HDPE, suggesting that the peat ash/ HDPE composites can be a potential automotive reinforce material.
- The higher tensile strengths and flexural modulus of the peat ash/ HDPE composites are highly dependent upon many factors, such as SA chemical treatment, ash loading and the use of MA-g-HDPE compatibilizer.
- A few barriers, such as low melt flow ability, high density and low impact property, may cause difficulty in the widespread, practical applications of these kind of polymer composites.

These technologies, if proved successful, can generate significant environmental and economic impacts to the reinforced material manufacturing and the automotive industries. They may also be harnessed to resolve the economic and environmental challenges faced by the peat ash producing industries.

#### 5. Acknowledgements

This work was supported by the Athlone Institute of Technology, Presidents Seed Fund and direct funding from Mergon International, Water Street, Castlepollard, Westmeath, Ireland.

#### 6. References

- [1] Kim JK, Lee HD, Kim HS, Park HY, Kim SC. Combustion possibility of low rank Russian peat as a blended fuel of pulverized coal fired power plant. *J Ind Eng Chem* 2013. doi:<http://dx.doi.org/10.1016/j.jiec.2013.08.027>.

- [2] Shao Y, Xu C, Zhu J, Preto F, Wang J, Tourigny G, et al. Ash and chlorine deposition during co-combustion of lignite and a chlorine-rich Canadian peat in a fluidized bed – Effects of blending ratio, moisture content and sulfur addition. *Fuel* 2012;95:25–34. doi:<http://dx.doi.org/10.1016/j.fuel.2011.12.020>.
- [3] Xu C, Donald J. Upgrading peat to gas and liquid fuels in supercritical water with catalysts. *Fuel* 2012;102:16–25. doi:<http://dx.doi.org/10.1016/j.fuel.2008.04.042>.
- [4] SEAI SEAOFI. Energy security in Ireland a statistical overview. 2011.
- [5] Backman R, Khalil R a., Todorovic D, Skreiberg O, Becidan M, Goile F, et al. The effect of peat ash addition to demolition wood on the formation of alkali, lead and zinc compounds at staged combustion conditions. *Fuel Process Technol* 2013;105:20–7. doi:[10.1016/j.fuproc.2011.04.035](http://dx.doi.org/10.1016/j.fuproc.2011.04.035).
- [6] Hytönen J. Effect of peat ash fertilization on the nutrient status and biomass production of short-rotation willow on cut-away peatland area. *Biomass and Bioenergy* 1998;15:83–92. doi:[http://dx.doi.org/10.1016/S0961-9534\(97\)10050-2](http://dx.doi.org/10.1016/S0961-9534(97)10050-2).
- [7] Korpjarvi K, Ryymin R, Saarno T, Reinikaiene M, Raisanen M. Utilisation of ashes from co-combustion of peat and wood- case study of a modern CFB- boiler in Finland. *Varmeforsk* 2012.
- [8] Dahl O, Nurmesniemi H, Pöykiö R, Watkins G. Comparison of the characteristics of bottom ash and fly ash from a medium-size (32 MW) municipal district heating plant incinerating forest residues and peat in a fluidized-bed boiler. *Fuel Process Technol* 2009;90:871–8. doi:<http://dx.doi.org/10.1016/j.fuproc.2009.04.013>.
- [9] Ahmaruzzaman M. A review on the utilization of fly ash. *Prog Energy Combust Sci* 2010;36:327–63. doi:<http://dx.doi.org/10.1016/j.pecs.2009.11.003>.
- [10] Shao Y, Wang J, Xu CC, Zhu J, Preto F, Tourigny G, et al. An experimental and modeling study of ash deposition behaviour for co-firing peat with lignite. *Appl Energy* 2011;88:2635–40. doi:[10.1016/j.apenergy.2011.02.006](http://dx.doi.org/10.1016/j.apenergy.2011.02.006).
- [11] Wang C, Wang D, Zheng S. Preparation of aluminum silicate/fly ash particles composite and its application in filling polyamide 6. *Mater Lett* 2013;111:208–10. doi:<http://dx.doi.org/10.1016/j.matlet.2013.08.110>.
- [12] Kim H, Biswas J, Choe S. Effects of stearic acid coating on zeolite in LDPE, LLDPE, and HDPE composites. *Polymer (Guildf)* 2006;47:3981–92. doi:<http://dx.doi.org/10.1016/j.polymer.2006.03.068>.
- [13] Yao N, Zhang P, Song L, Kang M, Lu Z, Zheng R. Stearic acid coating on circulating fluidized bed combustion fly ashes and its effect on the mechanical performance of polymer composites. *Appl Surf Sci* 2013;279:109–15. doi:<http://dx.doi.org/10.1016/j.apsusc.2013.04.045>.
- [14] Deepthi M V, Sharma M, Sailaja RRN, Anantha P, Sampathkumaran P, Seetharamu S. Mechanical and thermal characteristics of high density polyethylene–fly ash

Cenospheres composites. *Mater Des* 2010;31:2051–60.  
doi:<http://dx.doi.org/10.1016/j.matdes.2009.10.014>.

- [15] Wang C, Liu J, Du H, Guo A. Effect of fly ash cenospheres on the microstructure and properties of silica-based composites. *Ceram Int* 2012;38:4395–400.  
doi:<http://dx.doi.org/10.1016/j.ceramint.2012.01.044>.
- [16] Alfaro EF, Dias DB, Silva LGA. The study of ionizing radiation effects on polypropylene and rice husk ash composite. *Radiat Phys Chem* 2013;84:163–5.  
doi:<http://dx.doi.org/10.1016/j.radphyschem.2012.06.025>.
- [17] Garbacz A, Sokołowska JJ. Concrete-like polymer composites with fly ashes – Comparative study. *Constr Build Mater* 2013;38:689–99.  
doi:<http://dx.doi.org/10.1016/j.conbuildmat.2012.08.052>.
- [18] Steenari BM, Schelander S, Lindqvist O. Chemical and leaching characteristics of ash from combustion of coal, peat and wood in a 12&#xa0;MW CFB – a comparative study. *Fuel* 1999;78:249–58. doi:[http://dx.doi.org/10.1016/S0016-2361\(98\)00137-9](http://dx.doi.org/10.1016/S0016-2361(98)00137-9).
- [19] Tyni SK, Karppinen J a., Tiainen MS, Laitinen RS. Preparation and characterization of amorphous aluminosilicate polymers from ash formed in combustion of peat and wood mixtures. *J Non Cryst Solids* 2014;387:94–100. doi:10.1016/j.jnoncrysol.2013.12.032.
- [20] Brown PA, Gill SA, Allen SJ. Metal removal from wastewater using peat. *Water Res* 2000;34:3907–16. doi:[http://dx.doi.org/10.1016/S0043-1354\(00\)00152-4](http://dx.doi.org/10.1016/S0043-1354(00)00152-4).
- [21] Metin D, Tihminlioğlu F, Balköse D, Ülkü S. The effect of interfacial interactions on the mechanical properties of polypropylene/natural zeolite composites. *Compos Part A Appl Sci Manuf* 2004;35:23–32.
- [22] Sengupta S, Maity P, Ray D, Mukhopadhyay A. Stearic acid as coupling agent in fly ash reinforced recycled polypropylene matrix composites: Structural, mechanical, and thermal characterizations. *J Appl Polym Sci* 2013;130:1996–2004.  
doi:10.1002/app.39413.
- [23] Mohanty S, Verma SK, Nayak SK. Dynamic mechanical and thermal properties of MAPE treated jute/HDPE composites. *Compos Sci Technol* 2006;66:538–47.  
doi:10.1016/j.compscitech.2005.06.014.
- [24] Gao H, Xie Y, Ou R, Wang Q. Grafting effects of polypropylene/polyethylene blends with maleic anhydride on the properties of the resulting wood–plastic composites. *Compos Part A Appl Sci Manuf* 2012;43:150–7.  
doi:10.1016/j.compositesa.2011.10.001.
- [25] Pérez E, Alvarez V, Pérez CJ, Bernal C. A comparative study of the effect of different rigid fillers on the fracture and failure behavior of polypropylene based composites. *Compos Part B Eng* 2013;52:72–83.  
doi:<http://dx.doi.org/10.1016/j.compositesb.2013.03.035>.

- [26] Ayswarya EP, Vidya Francis KF, Renju VS, Thachil ET. Rice husk ash – A valuable reinforcement for high density polyethylene. *Mater Des* 2012;41:1–7. doi:<http://dx.doi.org/10.1016/j.matdes.2012.04.035>.
- [27] Atuanya CU, Edokpia RO, Aigbodion VS. The physio-mechanical properties of recycled low density polyethylene (RLDPE)/bean pod ash particulate composites. *Results Phys* 2014;4:88–95. doi:10.1016/j.rinp.2014.05.003.
- [28] Ooi ZX, Ismail H, Abu Bakar A. Curing characteristics, mechanical, morphological, and swelling assessment of liquid epoxidized natural rubber coated oil palm ash reinforced natural rubber composites. *Polym Test* 2014;33:145–51. doi:10.1016/j.polymertesting.2013.11.007.
- [29] Asuke F, Abdulwahab M, Aigbodion VS, Fayomi OSI, Aponbiede O. Effect of load on the wear behaviour of polypropylene/carbonized bone ash particulate composite. *Egypt J Basic Appl Sci* 2014;1:67–70. doi:10.1016/j.ejbas.2014.02.002.
- [30] Aigbodion VS, Hassan SB, Agunsoye JO. Effect of bagasse ash reinforcement on dry sliding wear behaviour of polymer matrix composites. *Mater Des* 2012;33:322–7. doi:10.1016/j.matdes.2011.07.002.
- [31] Dantungee R, Yun J, Supaphol P. Melt rheology and extrudate swell of calcium carbonate nanoparticle-filled isotactic polypropylene. *Polym Test* 2005;24:2–11.
- [32] Zhang Y, He P, Xu X, Li J. Use of atomic force microscopy for imaging the initial stage of the nucleation of calcium phosphate in langmuir-blodgett films of stearic acid. *Thin Solid Films* 2004;468:273–9. doi:10.1016/j.tsf.2004.06.153.
- [33] Chakradhar RPS, Dinesh Kumar V. Water-repellent coatings prepared by modification of ZnO nanoparticles. *Spectrochim Acta - Part A Mol Biomol Spectrosc* 2012;94:352–6. doi:10.1016/j.saa.2012.03.079.
- [34] Nath DCD, Bandyopadhyay S, Campbell J, Yu A, Blackburn D, White C. Surface-coated fly ash reinforced biodegradable poly(vinyl alcohol) composite films: part 2-analysis and characterization. *Appl Surf Sci* 2010;257:1216–21. doi:<http://dx.doi.org/10.1016/j.apsusc.2010.08.025>.
- [35] Divya VC, Ameen Khan M, Nageshwar Rao B, Sailaja RRN. High density polyethylene/cenosphere composites reinforced with multi-walled carbon nanotubes: Mechanical, thermal and fire retardancy studies. *Mater Des* 2015;65:377–86. doi:10.1016/j.matdes.2014.08.076.
- [36] Igarza E, Pardo SG, Abad MJ, Cano J, Galante MJ, Pettarin V, et al. Structure-fracture properties relationship for Polypropylene reinforced with fly ash with and without maleic anhydride functionalized isotactic Polypropylene as coupling agent. *Mater Des* 2013. doi:<http://dx.doi.org/10.1016/j.matdes.2013.09.055>.
- [37] Kuwahara Y, Yamashita H. A new catalytic opportunity for waste materials: Application of waste slag based catalyst in CO<sub>2</sub> fixation reaction. *J CO<sub>2</sub> Util* 2013;1:50–9. doi:<http://dx.doi.org/10.1016/j.jcou.2013.03.001>.

- [38] Satheesh Raja R, Manisekar K, Manikandan V. Study on mechanical properties of fly ash impregnated glass fiber reinforced polymer composites using mixture design analysis. *Mater Des* 2013. doi:<http://dx.doi.org/10.1016/j.matdes.2013.10.026>.
- [39] Zuiderduin WCJ, Westzaan C, Huétink J, Gaymans RJ. Toughening of polypropylene with calcium carbonate particles. *Polymer (Guildf)* 2003;44:261–75. doi:[http://dx.doi.org/10.1016/S0032-3861\(02\)00769-3](http://dx.doi.org/10.1016/S0032-3861(02)00769-3).
- [40] Guerreiro SDC, João IM, Pimentel Real LE. Evaluation of the influence of testing parameters on the melt flow index of thermoplastics. *Polym Test* 2012;31:1026–30. doi:<http://dx.doi.org/10.1016/j.polymertesting.2012.07.008>.
- [41] Guerrica-Echevarría G, Eguiazábal JI, Nazábal J. Influence of molding conditions and talc content on the properties of polypropylene composites. *Eur Polym J* 1998;34:1213–9. doi:[http://dx.doi.org/10.1016/S0014-3057\(97\)00228-0](http://dx.doi.org/10.1016/S0014-3057(97)00228-0).
- [42] Jikan SS, Arshat I M, Badarulzaman Nur. A. Melt Flow And Mechanical Properties Of Polypropylene/recycled Plaster Of Paris. *Appl Mech Mater* 2013;315:905–8. doi:[10.4028/www.scientific.net/AMM.315.905](http://dx.doi.org/10.4028/www.scientific.net/AMM.315.905).
- [43] Dhakal HN, Zhang Z, Nicolais L. *Polymer Matrix Composites: Moisture Effects and Dimensional Stability*. Wiley Encycl. Compos., John Wiley & Sons, Inc.; 2011. doi:[10.1002/9781118097298.weoc178](http://dx.doi.org/10.1002/9781118097298.weoc178).
- [44] Ma XF, Yu JG, Wang N. Fly ash-reinforced thermoplastic starch composites. *Carbohydr Polym* 2007;67:32–9. doi:<http://dx.doi.org/10.1016/j.carbpol.2006.04.012>.
- [45] Chaowasakoo T, Sombatsompop N. Mechanical and morphological properties of fly ash/epoxy composites using conventional thermal and microwave curing methods. *Compos Sci Technol* 2007;67:2282–91. doi:[10.1016/j.compscitech.2007.01.016](http://dx.doi.org/10.1016/j.compscitech.2007.01.016).
- [46] Lee S-Y, Yang H-S, Kim H-J, Jeong C-S, Lim B-S, Lee J-N. Creep behavior and manufacturing parameters of wood flour filled polypropylene composites. *Compos Struct* 2004;65:459–69. doi:<http://dx.doi.org/10.1016/j.compstruct.2003.12.007>.
- [47] Yang H-S, Kim H-J, Son J, Park H-J, Lee B-J, Hwang T-S. Rice-husk flour filled polypropylene composites; mechanical and morphological study. *Compos Struct* 2004;63:305–12. doi:[http://dx.doi.org/10.1016/S0263-8223\(03\)00179-X](http://dx.doi.org/10.1016/S0263-8223(03)00179-X).
- [48] Keener TJ, Stuart RK, Brown TK. Maleated coupling agents for natural fibre composites. *Compos Part A Appl Sci Manuf* 2004;35:357–62. doi:<http://dx.doi.org/10.1016/j.compositesa.2003.09.014>.
- [49] Ismail H, Shaari SM. Curing characteristics, tensile properties and morphology of palm ash/halloysite nanotubes/ethylene-propylene-diene monomer (EPDM) hybrid composites. *Polym Test* 2010;29:872–8. doi:<http://dx.doi.org/10.1016/j.polymertesting.2010.04.005>.



- [50] Liang J-Z, Duan D-R, Tang C-Y, Tsui C-P, Chen D-Z. Tensile properties of PLLA/PCL composites filled with nanometer calcium carbonate. *Polym Test* 2013;32:617–21. doi:<http://dx.doi.org/10.1016/j.polymertesting.2013.02.008>.
- [51] Dányádi L, Janecska T, Szabó Z, Nagy G, Móczó J, Pukánszky B. Wood flour filled PP composites: Compatibilization and adhesion. *Compos Sci Technol* 2007;67:2838–46. doi:10.1016/j.compscitech.2007.01.024.
- [52] Gunning MA, Istrate OM, Geever LM, Lyons JG, Blackie P, Chen B, et al. The effect of maleic anhydride grafting efficiency on the flexural properties of polyethylene composites. *J Appl Polym Sci* 2012;124:4799–808. doi:10.1002/app.35545.
- [53] Ahmed K, Raza NZ, Habib F, Aijaz M, Afridi MH. An investigation on the influence of filler loading and compatibilizer on the properties of polypropylene/marble sludge composites. *J Ind Eng Chem* 2013;19:1805–10. doi:<http://dx.doi.org/10.1016/j.jiec.2013.02.024>.
- [54] Gupta N, Singhbrar B, Woldesenbet E. Effect of filler addition on the compressive and impact properties of glass fibre reinforced epoxy. *Indian Acad Sci* 2001;24:219–23.
- [55] Hristov VN, Lach R, Grellmann W. Impact fracture behavior of modified polypropylene/wood fiber composites. *Polym Test* 2004;23:581–9. doi:<http://dx.doi.org/10.1016/j.polymertesting.2003.10.011>.
- [56] Parvaiz MR, Mohanty S, Nayak SK, Mahanwar PA. Effect of surface modification of fly ash on the mechanical, thermal, electrical and morphological properties of polyetheretherketone composites. *Mater Sci Eng A* 2011;528:4277–86. doi:10.1016/j.msea.2011.01.026.
- [57] Satapathy S, Nag A, Nando GB. Thermoplastic elastomers from waste polyethylene and reclaim rubber blends and their composites with fly ash. *Process Saf Environ Prot* 2010;88:131–41. doi:<http://dx.doi.org/10.1016/j.psep.2009.12.001>.
- [58] Rothon RN. *Particulate-Filled Polymer Composites* (2nd Edition). 2003.